



Supporting Online Material for

A Common Explosion Mechanism for Type Ia Supernovae

Paolo A. Mazzali,* Friedrich K. Röpke, Stefano Benetti, Wolfgang Hillebrandt

*To whom correspondence should be addressed. E-mail: mazzali@mpa-garching.mpg.de

Published 9 February 2007, *Science* **315**, 825 (2007)

DOI: 10.1126/science.1136259

This PDF file includes:

Figs. S1 to S5

Table S1

References

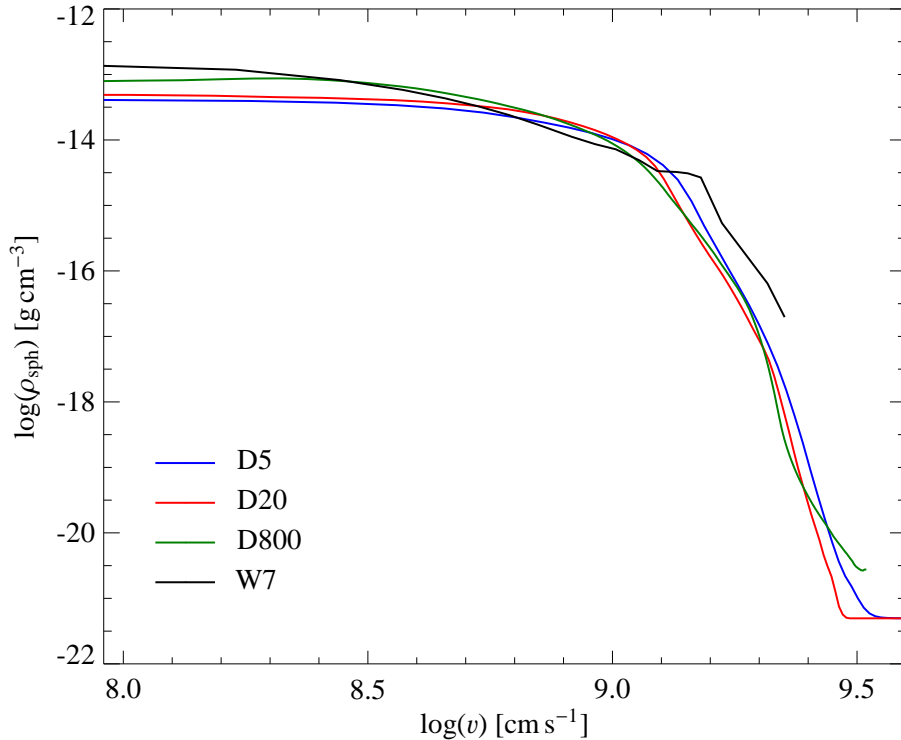


Figure 1: The density-velocity distribution of the standard, one-dimensional, Chandrasekhar-mass, deflagration explosion model W7(S1), and those of the three 3D delayed detonation models studied in this paper. The density distribution of W7 is different to those of other M_{Ch} 1D explosion models, and so adopting other models would not have a significant impact on the values of the masses derived in this paper. Our 3D delayed detonation models still suffer from a somewhat low production of energy as can be seen by the lack of material at the highest velocities. In a SN explosion, the velocity of a particular layer of the exploding star is set at the time of explosion and remains constant thereafter, therefore velocity and radius are linked as $R = vt$.

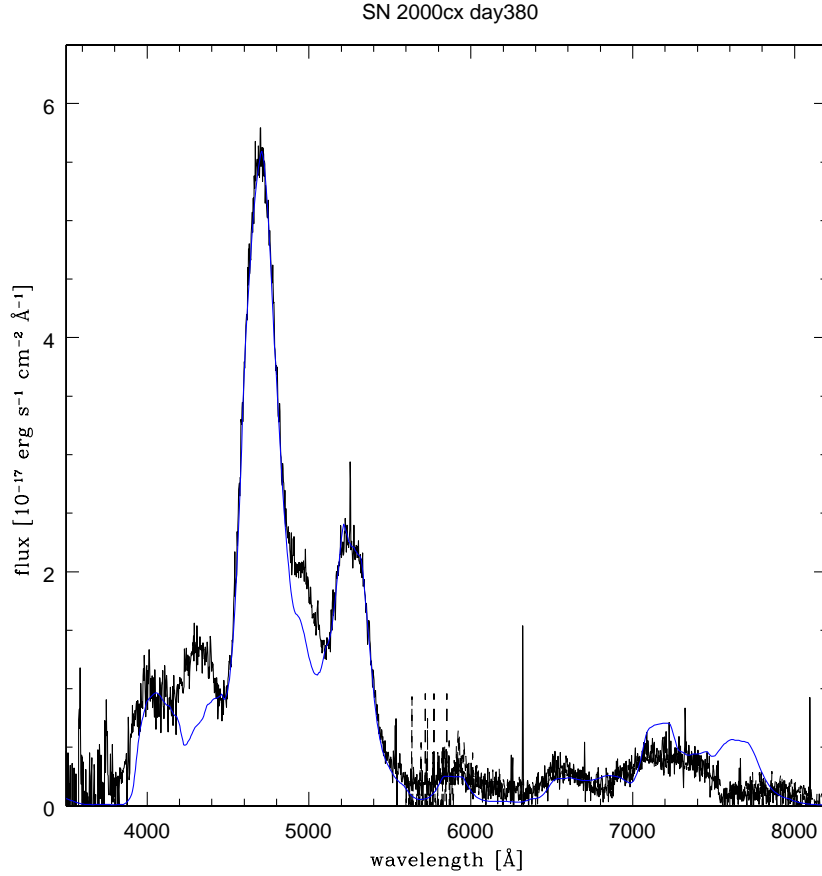


Figure 2: An example of a nebular spectrum fit: the case of the peculiar SN 2000cx. Although SN 2000cx does not conform with the relation between peak luminosity and decline rate, the nebular spectrum is fitted well with our assumption of a W7 density distribution. The spectrum is dominated by two strong emissions due mostly to forbidden lines of iron. The emission near 4700Å includes lines of both [Fe II] (strongest lines at 4814, 4890, and 4905Å) and [Fe III] (strongest lines at 4858 and 4701Å), while the other, near 5200Å, is due only to [Fe II] lines (strongest lines at 5159 and 5262Å). Fitting the strength and profiles two features simultaneously implies obtaining a good description of the ionization state of Fe throughout the SN ejecta. Since Fe is the dominant element, the ionization of the other elements can be expected also to be reasonably well described. The black line shows the observed spectrum, the blue line is the synthetic spectrum.

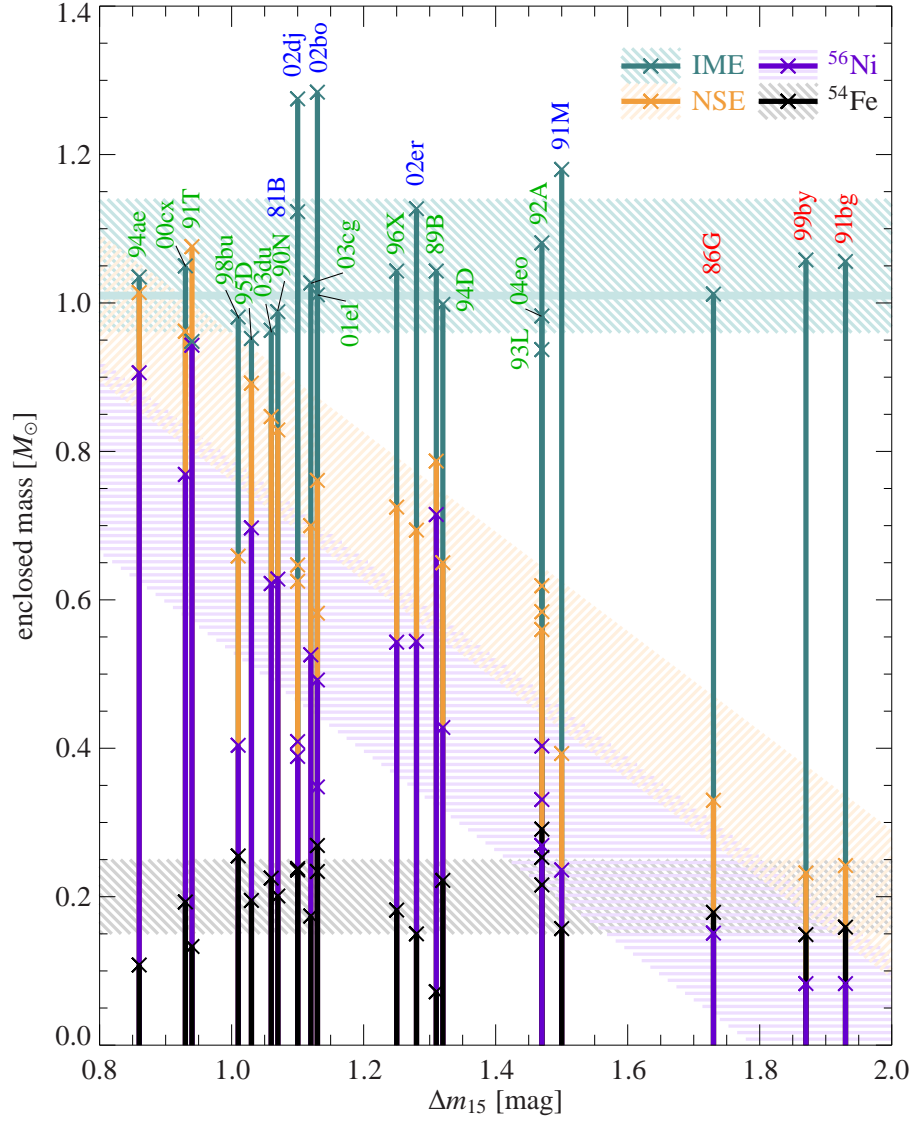


Figure 4: This plot is similar to the Zorro diagram (Fig.1, SI3) but now the SNe are plotted individually as vertical bars to make the individual components easier to read.

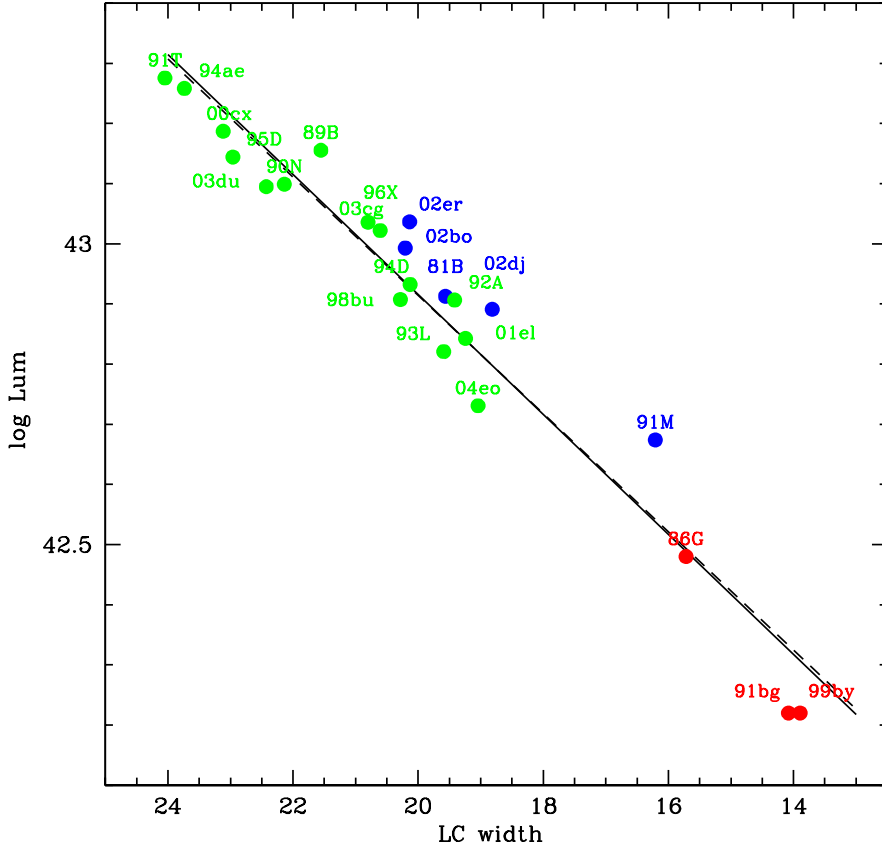


Figure 5: Observed and synthetic brightness-decline rate relation for the SNe in our sample. The peak luminosity L depends on the ^{56}Ni mass as $L = 2 \times 10^{43} M(^{56}\text{Ni})$. Synthetic light curve widths were obtained as follows: 1) The width of the light curve τ , which is related to the decline rate, depends on the ejected mass M_{ej} , the kinetic energy E_K , and the opacity κ as follows: $\tau \propto \kappa^{\frac{1}{2}} E_K^{-\frac{1}{4}} M_{\text{ej}}^{\frac{3}{4}}$. 2) The ejected mass is constant and equal to M_{Ch} , and the density distribution is given by W7. Other models give similar results. 3) The kinetic energy released in the explosion depends only weakly on whether burning is to NSE or to IME: $E_K = [1.56M(^{56}\text{Ni}) + 1.74M(\text{stable NSE}) + 1.24M(\text{IME}) - 0.46]10^{51}$ erg (S3). 4) The opacity was assumed to be mostly due to line absorption. This means that NSE elements contribute much more than IME, because they have a much more complex atomic level structure. The opacity was therefore parametrised on the basis of the abundances of the different isotopes and was computed using the formula $\kappa \propto M(\text{NSE}) + 0.1M(\text{IME})$. This yields parametrized bolometric light curve widths, which were compared to observed values as follows: 1) the value of the width of the observed bolometric light curves was obtained from the rise and decline times published in (S4) as $T = (t_{-1/2} + t_{+1/2})$. For those SNe where $t_{-1/2}$ is missing, it was estimated from the relation between $t_{-1/2}$ and $\Delta m_{15}(\text{B})$ derived from the other SNe. 2) For each of the 7 SNe that are common to our sample and that of (S4), a scale factor $x = T/\tau$ was then computed. The average value, 24.447, was applied to convert τ to time. Dots show the individual SNe. The dashed line is a linear regression between the SN luminosity derived as above and the LC width from (S4), for the 7 SNe common to both samples. The fully drawn line is a linear regression between the SN luminosity derived as above and the LC width determined from the abundances as discussed above for our sample of 23 SNe Ia.

Table 1: Supplementary Online Material: The supernova sample

SN	$\Delta m_{15}(B)^a$	$\langle \dot{v} \rangle$ [km · s ⁻¹ · d ⁻¹] ^a	logL [erg.s ⁻¹]	⁵⁶ Ni [M _⊙]
LVG				
89B	1.34 ± 0.07	66 ± 5	43.16	0.72 ± 0.10
90N	1.08 ± 0.05	41 ± 5	43.10	0.63 ± 0.05
91T	0.95 ± 0.05	11 ± 5	43.28	0.94 ± 0.05
92A	1.47 ± 0.05	45 ± 5	42.91	0.40 ± 0.05
93L ^b	1.50 ± 0.30	32 ± 10	42.82	0.33 ± 0.05
94D	1.32 ± 0.05	39 ± 5	42.93	0.43 ± 0.08
94ae ^b	0.88 ± 0.10	43 ± 5	43.26	0.91 ± 0.05
95D ^b	1.04 ± 0.05	18 ± 5	43.14	0.70 ± 0.07
96X	1.26 ± 0.05	46 ± 5	43.04	0.54 ± 0.05
98bu	1.04 ± 0.05	10 ± 5	42.91	0.40 ± 0.05
00cx ^b	0.94 ± 0.05	2 ± 5	43.19	0.77 ± 0.05
01el	1.15 ± 0.04	31 ± 5	42.84	0.35 ± 0.05
03cg ^c	1.25 ± 0.05	38 ± 6	43.02	0.53 ± 0.05
03du	1.06 ± 0.06	31 ± 5	43.09	0.62 ± 0.05
04eo	1.48 ± 0.04	45 ± 4	42.73	0.27 ± 0.05
HVG				
81B	1.11 ± 0.07	76 ± 7	42.91	0.41 ± 0.05
91M	1.51 ± 0.10	92 ± 5	42.67	0.24 ± 0.05
02bo	1.17 ± 0.05	110 ± 7	42.99	0.49 ± 0.05
02dj	1.11 ± 0.05	86 ± 6	42.89	0.39 ± 0.05
02er	1.32 ± 0.04	92 ± 5	43.04	0.54 ± 0.05
FAINT				
86G	1.78 ± 0.07	64 ± 5	42.48	0.15 ± 0.05
91bg	1.93 ± 0.10	104 ± 7	42.22	0.08 ± 0.03
99by	1.87 ± 0.10	110 ± 10	42.22	0.08 ± 0.03

^a Values from (S5), which is mostly based on the SN sample of (S2), unless otherwise stated.

$\Delta m_{15}(B)$ values are reddening corrected according to (S6).

^b Not in (S5); photometric parameters are from (S7)

^c Not in (S5); photometric parameters are from (S8)

SOM References

- S1. K. Nomoto, F.-K. Thielemann, K. Yokoi, *ApJ* 286, 644 (1984).
- S2. S. Benetti, et al., *ApJ* 623, 1011 (2005).
- S3. S.E. Woosley, D. Kasen, S. Blinnikov, E. Sorokina, *ArXiv Astrophysics e-prints astro-ph/0609562* (2006).
- S4. G. Contardo, B. Leibundgut, W.D. Vacca, *A&A* 359, 876 (2000).
- S5. S. Hachinger, P.A. Mazzali, S. Benetti, *MNRAS* 370, 299 (2006).
- S6. M.M. Phillips, P. Lira, N. Suntzeff, R.R. Schommer, M. Hamuy, J. Maza, *AJ* 118, 1766 (1999).
- S7. G. Altavilla, et al., *MNRAS* 349, 1344 (2004).
- S8. N. Elias-Rosa, et al., *MNRAS* 369, 1880 (2006).